Attenuation of the Aggregation and Neurotoxicity of Amyloid-β Peptides by Catalytic Photooxygenation**

Atsuhiko Taniguchi, Daisuke Sasaki, Azusa Shiohara, Takeshi Iwatsubo, Taisuke Tomita, Youhei Sohma, and Motomu Kanai**

Abstract: *Alzheimer's disease (AD), a progressive severe neurodegenerative disorder, is currently incurable, despite intensive efforts worldwide. Herein, we demonstrate that catalytic oxygenation of amyloid-β peptides (Aβ) might be an effective approach to treat AD. Aβ1–42 was oxygenated under physiologically-relevant conditions (pH 7.4, 37°C) using a riboflavin catalyst and visible light irradiation, with modifications at the Tyr10, His13, His14, and Met35 residues. The oxygenated Aβ1–42 exhibited considerably lower aggregation potency and neurotoxicity compared with native Aβ. Photooxygenation of Aβ can be performed even in the presence of cells, by using a selective flavin catalyst attached to an Aβ-binding peptide; the Aβ cytotoxicity was attenuated in this case as well. Furthermore, oxygenated Aβ1–42 inhibited the aggregation and cytotoxicity of native Aβ.*

Amyloid-β peptides (Aβ), comprised mainly of 40- and 42-residue peptides (designated Aβ1–40 and Aβ1–42, respectively), are widely considered the primary pathogens underlying Alzheimer's disease (AD), a severe neurodegenerative disorder present mostly in the elderly population.[1] Senile plaques in the brain, one of the pathological hallmarks of AD, are formed by the accumulation of aggregated Aβ with an extensive β-sheet structure. The aggregation process of monomer Aβ to oligomers and successively to fibrils is strongly associated with the onset of neurotoxicity. Although Aβ1–40 is the predominant product, Aβ1–42 is far more aggregative and neurotoxic.[2,3]

In this context, therapeutic approaches targeting the pathological properties of Aβ might be promising to overcome AD.[4] For example, inhibition of β- and γ-secretases responsible to Aβ production, modulation of Aβ aggregation, and anti-Aβ immunotherapies are considered candidates for AD treatments. None of these approaches has yet to be applied clinically, however, and further development of Aβ-targeted approaches is needed.

We envisioned that cell-compatible, artificial chemical transformation of toxic, aberrant Aβ to less toxic forms at the disease site might be an alternative candidate for Aβ-targeted AD treatment. For chemical transformations of Aβ, hydrolysis using a cobalt(III)–cyclen complex[5] and UV photodegradation using a fullerene–glucose conjugate[6,7] were reported. We selected riboflavin (vitamin B2)-catalyzed photooxygenation of Aβ with visible light as a target chemical transformation (Figure 1a).[8–10] The potential advantages of riboflavin-catalyzed photooxygenation of Aβ would be: 1) tolerance to aqueous media using molecular oxygen as the sole oxidant,[9] 2) low toxicity of riboflavin as an organocatalyst, and 3) the possibility of on/off control by irradiation with harmless visible light. As reactive oxygen species are generally poisonous if diffused from the target molecule,[11] catalytic oxidation using short-lived oxygenation species with secured Aβ-selectivity is indispensable for the success of this novel therapeutic approach.

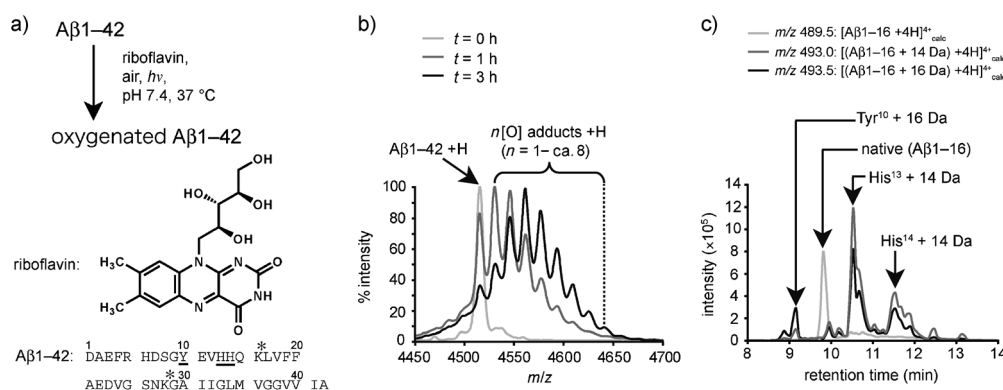A phosphate buffer solution (pH 7.4) containing Aβ1–42 (20 μm; generated from the *O*-acyl isopeptide)[12] and riboflavin (20 mol%) was irradiated using a fluorescent lamp at 37°C (Figure 1a), and the reaction was monitored by matrix-assisted laser desorption ionization time-of-flight mass spectrometry (MALDI-TOF MS; Figure 1b) at arbitrary time points (t). MS intensities derived from the oxygen atom (n[O])-adducts ($n = 1$–3) of Aβ1–42 were relatively high at $t = 1$ h, and n[O]-adducts ($n = 1$–8) were detected at $t = 3$ h at the expense of the native form of Aβ1–42. In contrast, oxygenation did not proceed in the absence of riboflavin or light (Supporting Information, Figure S1). In amino acid analyses (Figure S2), the amounts of Tyr, Met, and His residues in the oxygenated sample decreased to approximately half to one-third of those in the non-oxygenated sample (native Aβ1–42). Instead, the amount of Met(O) was increased in the oxygenated sample.

[*] Dr. A. Taniguchi, Dr. D. Sasaki, A. Shiohara, Prof. T. Iwatsubo, Dr. T. Tomita, Dr. Y. Sohma, Prof. M. Kanai
Graduate School of Pharmaceutical Sciences, The University of Tokyo, Bunkyo-ku, Tokyo 113-0033 (Japan)
E-mail: ysohma@mol.f.u-tokyo.ac.jp
          kanai@mol.f.u-tokyo.ac.jp

Dr. A. Taniguchi, Dr. D. Sasaki, Dr. Y. Sohma, Prof. M. Kanai
Japan Science and Technology Agency (JST), ERATO, Kanai Life Science Catalysis Project, Bunkyo-ku, Tokyo 113-0033 (Japan)

Prof. T. Iwatsubo
Graduate School of Medicine, The University of Tokyo
Bunkyo-ku, Tokyo 113-0033 (Japan)

Figure 1. Catalytic oxygenation of Aβ1–42 and product identification. a) Phosphate buffer solution (pH 7.4) containing Aβ1–42 (20 μM) and riboflavin (20 mol%) was irradiated by a fluorescent lamp at 37°C under air atmosphere. Confirmed oxygenated amino acid residues are underlined in the amino acid sequence. *=Scissile bonds by endoproteinase Lys-C. b) MALDI-TOF MS spectra of the reaction mixture at arbitrary time points (*t*). c) LC/MS/MS (ESI-Q-TOF) analysis of the Aβ1–16 fragments, generated by Lys-C digestion of the oxygenated Aβ1–42 (*t*=3 h at RT). Extracted ion chromatogram for the *m/z* of precursor ions whose structures were interpreted by MS/MS analysis. The results of MS/MS analysis of each peak indicated that a +16 Da modification occurred at Tyr10, a +14 Da at His13, and a +14 Da at His14 (for MS/MS spectra, see Figure S3 d–g). The peaks of +16 Da (——) at retention time=10.6 min and 11.5 min correspond to isotopic ions of the +14 Da products. LC conditions: C18 reverse-phase column (100×1.0 mm, 40°C) with a binary solvent system: linear gradient of 2–42% acetonitrile in 0.1% aqueous formic acid over 20 min at a flow rate of 20 μL min⁻¹.

To gain more detailed information about the oxygenated structures, oxygenated Aβ1–42 (*t*=3 h) was digested to three fragments, Aβ1–16, Aβ17–28, and Aβ29–42, using endoproteinase Lys-C (scissile bonds are indicated by an asterisk in the Aβ1–42 sequence in Figure 1a). MALDI-TOF MS was used to analyze the digested mixture (Figure S3a). The fragment Aβ17–28 remained intact, suggesting that no oxygenation occurred in the Aβ17–28 region. Aβ29–42 was not detected by MALDI MS, probably owing to its poor ionizability. On the other hand, *n*[O]-adducts (*n*=1–ca. 6) were detected from the Aβ1–16 fragment. Further analysis using electrospray ionization-quadrupole-time-of-flight (ESI-Q-TOF) LC/MS/MS revealed that a +16 Da modification occurred at the Tyr10 residue, probably yielding 3,4-dihydroxyphenylalanine (DOPA),[13] and a +14 Da modification occurred at the His13 and His14 residues, probably yielding a dehydro-2-imidazolone derivative[14] (Figure 1c; see also S3 b–g). Based on the MS, amino acid composition analyses, and LC/MS/MS analyses, Aβ1–42 was mainly converted into oxygenated forms at *t*=3 h, where oxygenation proceeded at one or more of the three types of amino acid residues (Tyr, His, or Met).[15]

The effect of oxygenative modification of Aβ1–42 on its aggregation properties was next examined using a thioflavin-T (ThT) dye assay (Figure 2a), the fluorescence intensity of

which increases with as the amyloid aggregation increases (generating a cross β-sheet).[16] A phosphate buffer solution (pH 7.4) containing Aβ1–42 (20 μM) and riboflavin (20 mol%) was incubated at 37°C with light irradiation (designated as oxygenated) or without irradiation (designated as native), and the incubation samples were analyzed at arbitrary time points (*t*). ThT fluorescence intensities of the oxygenated Aβ were remarkably lower than those of the native Aβ at *t*=3 h and 6 h, which suggests that the oxygenated Aβ did not form cross β-sheet-type aggregates.[17] In addition, atomic force microscopy analyses of the native and oxygenated samples after 6 h of incubation revealed that native Aβ formed robust fibrils, whereas oxygenated Aβ did not (Figure 2b). Dynamic light scattering and size exclusion chromatography also supported the formation of smaller assemblies of the oxygenated Aβ than the native Aβ (Figure S4). Furthermore, the oxygenated Aβ showed a random coil structure at *t*=6 h (verified by circular dichroism spectrometry), whereas the native Aβ adopted a β-sheet structure (negative maximum at 218 nm) after incubation for 6 h (Figure 2c). Thus, oxygenation prevented the conformational transition of Aβ from a random coil to a β-sheet. The riboflavin-catalyzed photooxygenation of partially aggregated Aβ, composed mainly of oligomer/protofibril species, also proceeded efficiently, and the aggregation potency of oligomer/protofibril Aβ to fibril was almost completely abolished by the oxygenation (Figure S5). Even Aβ in the fibril state underwent riboflavin-catalyzed photooxygenation (Figure S6). Overall, riboflavin-catalyzed photooxygenation
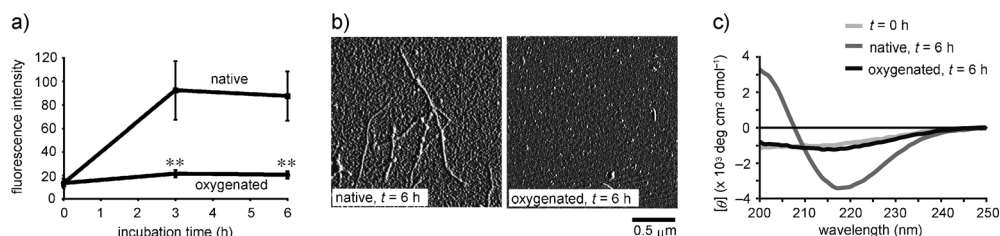
Figure 2. Aggregation properties of the native and oxygenated Aβ1–42. A phosphate buffer solution (pH 7.4) containing Aβ1–42 (20 μM) and riboflavin (20 mol%) was incubated at 37°C without light irradiation (designated as native) or with light irradiation (designated as oxygenated), and the incubation samples were analyzed at arbitrary time points (*t*). a) Thioflavin-T fluorescence assay (*n*=6, mean ±SD; **p<0.01 vs. native Aβ1–42 by Student's *t*-test). b) Atomic force microscopy shown in amplitude mode. c) Circular dichroism spectroscopy.

markedly attenuated the aggregation properties of monomeric and oligomeric/protofibril native Aβ.

We then examined the effects of riboflavin-catalyzed photooxygenation of Aβ on neurotoxicity. Rat cortical primary neurons were treated with native or oxygenated Aβ1–42 (10 μM each) for 72 h, and conditioned medium and cell lysates were analyzed (Figure S8). A lactase dehydrogenase (LDH) assay, in which the degree of LDH release is proportional to the number of dead cells, indicated that oxygenated Aβ had a remarkably lower cytotoxicity than native Aβ (Figure S8a). The lower toxicity of oxygenated Aβ was also supported by the results of experiments using rat pheochromocytoma PC12 cells (Figure S9). In addition, whereas synapses were damaged by the native Aβ, which was verified by the declined expression level of postsynaptic density protein (PSD) 95,[18] the oxygenated Aβ did not affect its expression level (Figure S8b,c). Thus, the neurotoxicity of the oxygenated Aβ was considerably lower than that of the native Aβ.

Moreover, photooxygenation by a flavin catalyst attached to an Aβ-binding peptide (2; Figure 3) was compatible with living cells, and diminished the toxicity of Aβ, even in the presence of the cells. To achieve selective Aβ oxygenation, we adopted a riboflavin analogue conjugated with a Lys[16]-Leu[17]-Val[18]-Phe[19]-Phe[20] (KLVFF)[19] derivative as an Aβ-binding tag. As the binding affinity of KLVFF itself was marginal, we

performed intensive structural optimization on it, which led us to identify D-[Lys-Leu-Val-Phe(4-phenyl)-Phe] as a ca. five-fold more potent aggregation inhibitor (a higher-affinity binder) than the parent KLVFF (Figure S10a). We also confirmed that the attachment of the flavin moiety did not affect the inhibitory activity. Thus, a phosphate-buffered saline solution containing Aβ (20 μM) and a catalyst (riboflavin (1): 4 μM, or 2: 20 μM) in PC12-cell-seeded wells was irradiated ($\lambda = 500$ nm) for 15 min at 37 °C under a 5 % CO_2 atmosphere. Both catalysts 1 and 2 oxygenated Aβ to a similar extent (approximately 65 %; Figure S10b) under these conditions.[20] After photooxygenation, an equal volume of culture medium was added to the wells (final Aβ species: 10 μM), the cells were incubated at 37 °C under a 5 % CO_2 atmosphere for 48 h, and the cell viabilities were measured (Figure 3). When catalyst 1 was used with photoirradiation, most of the cells died, irrespective of the presence or absence of Aβ (samples f and h) owing to nonselective oxidative damage to the cells. Using catalyst 2, however, more than half of the cells were alive after photoirradiation in the absence of Aβ (sample j). The lower phototoxicity of catalyst 2 than catalyst 1 is likely due to their relative oxygenation activities. Using catalyst 2 in the presence of Aβ, the cell viability under photoirradiation was significantly higher than that without photoirradiation (sample k vs. l). In sample l, inhibition of Aβ aggregation by the peptide moiety of 2 should partly contribute to the increased cell viability. This effect, however, proved to be minor compared to the effects of photooxygenation (compare samples c, k, and l). Thus, Aβ-selective photooxygenation in the presence of the cells to attenuate the Aβ toxicity was achieved using catalyst 2, which generates active oxidant(s) selectively at the positions proximate to Aβ.

Finally, we examined whether oxygenated Aβ1–42 affects the aggregation and toxicity of native Aβ1–42. When oxygenated Aβ1–42 was added to a freshly prepared solution containing native Aβ1–42 (20 μM each) and incubated at 37 °C, fewer long amyloid fibrils were observed than with Aβ1–42 alone (Figure S11a); this suggests that the oxygenated Aβ species inhibited the aggregation of native Aβ. The aggregation inhibitory activity of oxygenated Aβ was also supported by dynamic light scattering analysis, which showed that the main particle size distribution observed in Aβ1–42 alone (ca. 7000 nm) shifted to 20–50 nm following co-incubation with oxygenated Aβ (Figure S11b). Furthermore, PC12 cell viability following treatment with 10 μM native Aβ alone was only 20 % (sample c; Figure 4), whereas over 60 % of the cells survived following co-incubation with 10 μM oxygenated Aβ (sample d). A concentration-dependent inhibition by oxygenated Aβ was observed (61.3 % viability at 10 μM, 33.5 % at 3 μM, and 22.0 % at 1 μM). Thus, both the aggregation potency and the cytotoxicity of native Aβ were significantly suppressed by co-treatment with oxygenated Aβ.

In conclusion, we have demonstrated that Aβ1–42 was oxygenated by a riboflavin catalyst through with visible light irradiation under physiological conditions. Modifications at the Tyr[10], His[13], His[14] and Met[35] residues were identified based on enzymatic digestion-MS/MS and amino acid analyses. Specifically, it is noteworthy that photooxygenation of Aβ was possible even in the presence of cells by the use of a selective
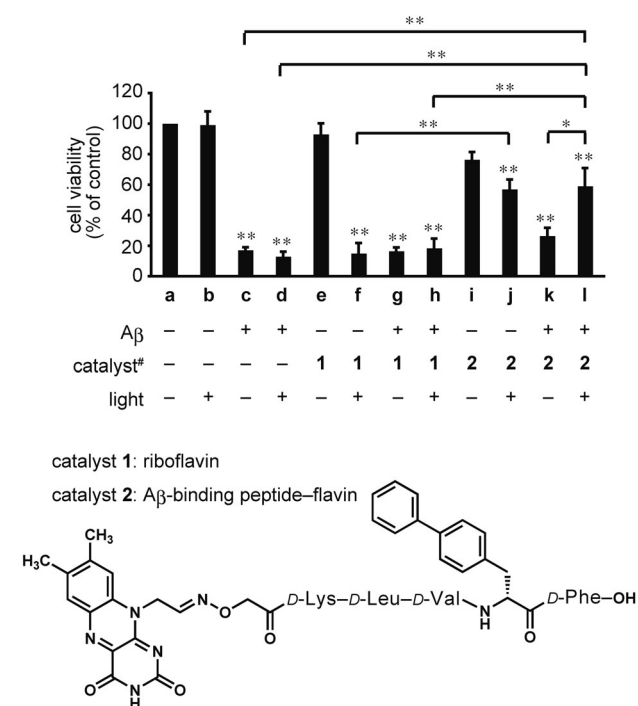
Figure 3. Photooxygenation in the presence of PC12 cells. Phosphate-buffered saline containing Aβ (20 μM) and catalyst (riboflavin: 4 μM, or 2: 20 μM) was irradiated with a light-emitting diode ($\lambda = 500$ nm) for 15 min at 37 °C under a 5 % CO_2 atmosphere in PC12-cell-seeded wells, then doubly diluted with culture medium (final Aβ species: 10 μM) and incubated at 37 °C under a 5 % CO_2 atmosphere for 48 h, and then applied to the cell viability assay ($n = 5$, mean ±SEM; $*p < 0.05$, $**p < 0.01$ vs. sample **a**, or in the indicated pair by Tukey's test).
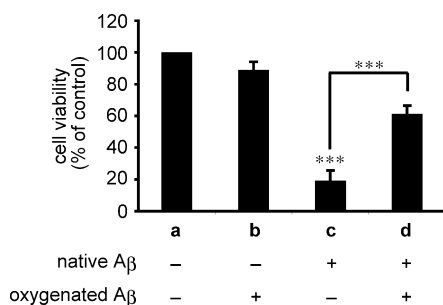
Figure 4. Effect of oxygenated Aβ1–42 on the cytotoxicity of native Aβ1–42. PC12 cells were treated with samples **a–d** (**a**: no Aβ species, **b**: 10 μM oxygenated Aβ [$t = 3$ h at RT], **c**: 10 μM native Aβ, **d**: 10 μM native Aβ + 10 μM oxygenated Aβ) for 48 h, and analyzed by cell viability assay ($n = 6$, mean ± SEM; ***$p < 0.001$ versus sample **a** or in the indicated pair by Tukey's test).

flavin catalyst attached to an Aβ-binding peptide. Oxygenation of Aβ induced two favorable features for the treatment of AD. First, the pathological properties of native Aβ, aggregation potency and neurotoxicity, were markedly attenuated by oxygenation. Second, the oxygenated Aβ inhibited the aggregation and cytotoxicity of native Aβ. Thus, riboflavin-catalyzed photooxygenation of Aβ not only decreases the concentration of aggregative and pathogenic natural Aβ, but also increases the concentration of an aggregation inhibitor (oxygenated Aβ1–42). As a next step, further development is required for application of this approach as a realistic treatment strategy for currently incurable AD, specifically the development of biologically benign catalytic conditions that lead to higher reactivity with the use of longer wavelength visible light, or even near-infrared light, which can penetrate bones of the skull, and higher Aβ-selectivity. Studies to overcome these hurdles and extension of the basic concept to the treatment of other diseases are ongoing in our group.

[1] D. M. Holtzman, J. C. Morris, A. M. Goate, *Sci. Transl. Med.* **2011**, *3*, 77sr1.

[2] T. Iwatsubo, A. Odaka, N. Suzuki, H. Mizusawa, N. Nukina, Y. Ihara, *Neuron* **1994**, *13*, 45–53.

[3] S. G. Younkin, *Ann. Neurol.* **1995**, *37*, 287–288.

[4] I. W. Hamley, *Chem. Rev.* **2012**, *112*, 5147–5192.

[5] J. Suh, S. H. Yoo, M. G. Kim, K. Jeong, J. Y. Ahn, M. Kim, P. S. Chae, T. Y. Lee, J. Lee, J. Lee, Y. A. Jang, E. H. Ko, *Angew. Chem.* **2007**, *119*, 7194–7197; *Angew. Chem. Int. Ed.* **2007**, *46*, 7064–7067.

[6] Y. Ishida, S. Tanimoto, D. Takahashi, K. Toshima, *Med. Chem. Commun.* **2010**, *1*, 212–215.

[7] Y. Ishida, T. Fujii, K. Oka, D. Takahashi, K. Toshima, *Chem. Asian J.* **2011**, *6*, 2312–2315.

[8] S. Fukuzumi, K. Tanii, T. Tanaka, *J. Chem. Soc. Chem. Commun.* **1989**, 816–818.

[9] R. Cibulka, R. Vasolid, B. König, *Chem. Eur. J.* **2004**, *10*, 6223–6231.

[10] J. Daďová, E. Svobodová, M. Sikorski, B. König, R. Cibulka, *ChemCatChem* **2012**, *4*, 620–623.

[11] On a relevant note, the relationship among metal ions, Aβ, and oxidative stress is discussed in Ref. [4]; see also: G. Eskici, P. H. Axelsen, *Biochemistry* **2012**, *51*, 6289–6311.

[12] A. Taniguchi, Y. Sohma, Y. Hirayama, H. Mukai, T. Kimura, Y. Hayashi, K. Matsuzaki, Y. Kiso, *ChemBioChem* **2009**, *10*, 710–715.

[13] D. I. Pattison, A. S. Rahmanto, M. J. Davies, *Photochem. Photobiol. Sci.* **2012**, *11*, 38–53.

[14] K. L. Schey, E. L. Finley, *Acc. Chem. Res.* **2000**, *33*, 299–306.

[15] Considering the presumably different ionizability of native vs. oxygenated Aβ and monomer vs. assembled Aβ, the MALDI MS spectra (Figure 1b) might not quantitatively reflect the efficacy of oxygenation. Nevertheless, based on the results of amino acid analysis (Figure S2) and LC/MS/MS study (Figure 1c), we conclude that Aβ1–42 was mainly converted into oxygenated forms after the reaction.

[16] H. LeVine III, *Methods Enzymol.* **1999**, *309*, 274–284.

[17] The aggregation potency of Aβ markedly decreased when only the Tyr[10] residue was selectively oxygenated to DOPA using tyrosinase (Figure S7). The result suggests that photooxygenation of Tyr[10] significantly contributes to the reduced aggregation potency of photooxygenated Aβ. In addition, an oxygenated Aβ derivative comprised of a sulfoxide form of the Met[35] residue was reported to possess lower aggregation potency and toxicity relative to wild-type Aβ; see: D. A. Butterfield, D. Boyd-Kimball, *Biochim. Biophys. Acta Proteins Proteomics* **2004**, *1703*, 149–156.

[18] K. H. Gylys, J. A. Fein, F. Yang, D. J. Wiley, C. A. Miller, G. M. Cole, *Am. J. Pathol.* **2004**, *165*, 1809–1817.

[19] L. O. Tjernberg, J. Näslund, F. Lindqvist, J. Johansson, A. R. Karlström, J. Thyberg, L. Terenius, C. Nordstedt, *J. Biol. Chem.* **1996**, *271*, 8545–8548.

[20] Catalyzed photooxygenation in a culture medium (including 0.1% horse serum) was less efficient than that in a phosphate buffer, probably because the reactive oxygen species generated reacted with the medium components.